

# STAP BASED GROUND MOVING TARGET DETECTABILITY IN THE AIRBORNE/SPACEBORNE ARRAY RADAR

*Jung S. Jung, Young K. Kwag*

Ocean Satellite Research Group  
Korea Ocean Research & Development Institute  
1270, Sa-2-dong, Sangrok-gu, Ansan-city, 426-744, Korea  
Radar Signal Processing Lab.  
Department of Avionics, Korea Aerospace University, Seoul, Korea  
E-mail: ykwag@kau.ac.kr

## 1. INTRODUCTION

A ground moving target indication (GMTI) technique can be used for providing the position and velocity of ground moving targets on moving platform. Recently, this technique has been known to have a possibility of the traffic monitoring of moving vehicle targets on the road by characterizing the dynamics of moving vehicles against a non-moving clutter background [1]. A STAP is a two-dimensional and adaptive signal processing technique for discriminating targets from clutter and jamming in moving platform [2]. A STAP can remove the ground clutter background efficiently, but it is difficult to detect the slow moving target in clutter rejection processing. In this paper, the probability of ground moving target detection is investigated in terms of the SNR and the detectable velocity of the ground target using STAP algorithm. And simulation results are presented with the clutter/jammer rejection performance and the probability of moving target detection in terms of SNR and MDV in the various false alarm rates.

## 2. CHARACTERISTICS OF RECEIVED ARRAY SIGNAL

Doppler frequency of moving target is determined by the radial target velocity which is given by the target-radar geometry. The received signal of ground moving target is represented by the function of azimuth angle,  $\varphi_i$ , which can be derived in (1)

$$s_i(\varphi) = A_i \exp\left[j \frac{2\pi}{\lambda} \times (2v_{rad} mT + (x_i \cos \varphi_i + y_i \sin \varphi_i) \cos \theta - z_i \sin \theta)\right] \quad (1)$$
$$i = 1, \dots, N, m = 1, \dots, M$$

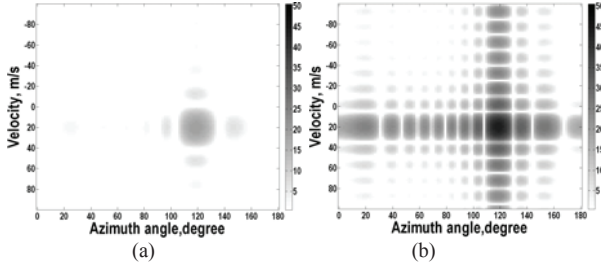


**Figure 1. Ground target response**

(a) N=8, M=8, SNR =20 dB, (b) N=12, M=12, SNR=45 dB

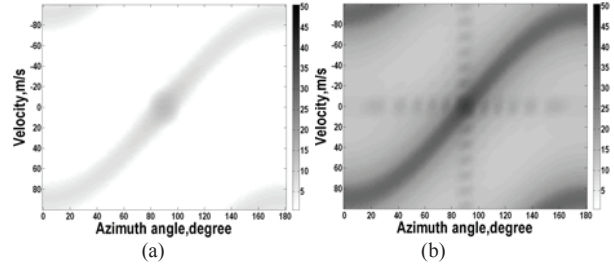


**Figure 2. Ground clutter spectrum.**

(a) N=8, M=8, SNR =20 dB, (b) N=12, M=12, SNR=45

where  $v_{rad}$  is radial velocity between platform and ground moving target. The ground target spectrum response is shown in Fig 1. Fig 1 (a) presents the moving target response when the SNR is 20dB and its velocity is 20 m/s, which is located at the degrees of 120 in azimuth direction. The array radar platform is assumed to move at the speed of 90 m/s in  $x$ -direction, and the number of antenna and coherent pulse is assumed to be eight, respectively. Fig 1 (b) shows the target response when SNR is 45 dB, and the number of antenna and coherent pulse is assumed to be eight, respectively. It is noted that the azimuth resolution is improved as the number of array antenna,  $N$ , is increased, and that Doppler resolution is improved as the number of pulse integration,  $M$ , is increased. In addition, the sidelobe effect in angle-Doppler plane is increased as the SNR of the target is increased.

For analyzing space-time processing algorithms, ground clutter is generated to complex signal due to train of coherent transmit pulse and array antenna [2]. Since the ground clutter signal is generated by the individual Doppler component cording to the azimuth angle, it can be represented in (2):

$$\begin{aligned}
 s_c &= \int_{\varphi}^{2\pi} A_c D(\varphi) L(\varphi) G(\varphi, m) \Phi_m(v_p, \varphi) \Psi_i(\varphi) d\varphi \\
 \Phi_m(v_p, \varphi) &= \exp[j \frac{2\pi}{\lambda} 2v_p m T \cos \varphi \cos \theta] \\
 \Psi_i(\varphi) &= \exp[j \frac{2\pi}{\lambda} ((x_i \cos \varphi + y_i \sin \varphi) \cos \theta - z_i \sin \theta)]
 \end{aligned} \tag{2}$$

where  $A_c$  is clutter amplitude and distribution,  $D$  is the sensor pattern,  $L$  is the ground reflectivity,  $G$  is the transmit directivity pattern, and  $\Phi_m$  and  $\Psi_i$  are the temporal and spatial phase term respectively. Ground clutter spectrum for a side-looking array is illustrated in Fig 2. Ground clutter spectrum extends from the upper right to the lower left corner. The maximum power of returned ground clutter signal appears at 90 degrees in azimuth and 0 m/s in Doppler so that sidelobe effect is maximized at this point.

Continuous wave noise jammer signal received by the  $i$ -th sensor of the array at the time  $m$  due to  $J$  jammers is represented in (3):

$$s_j = \sum_{j=1}^J A_j(m) \exp[j \frac{2\pi}{\lambda} \times ((x_i \cos \varphi_j + y_i \sin \varphi_j) \cos \theta_j - z_i \sin \theta_j)] \tag{3}$$

where  $A_j$  is the jammer amplitude,  $\varphi_j$  and  $\theta_j$  are the angles that determine the directions of the jammers.

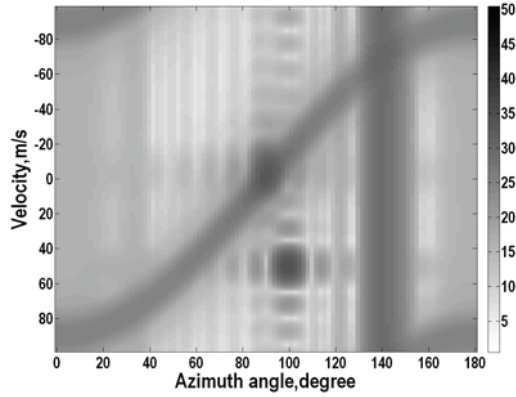


Figure 3. Simulation environment

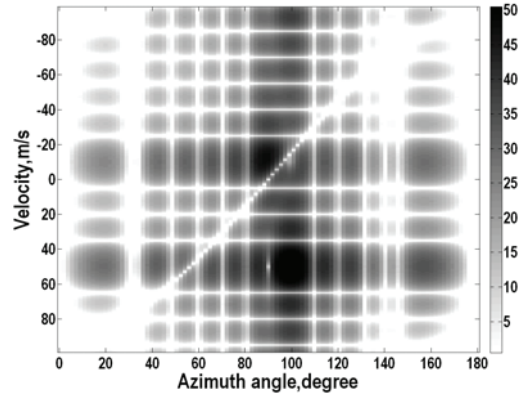


Figure 4. STAP output spectrum

TABLE I. Simulation Parameter

| System parameter               | value  | Environment parameter                     | value   |
|--------------------------------|--------|---|---------|
| Operating frequency            | 10 GHz | CNR                                       | 40 dB   |
| PRF                            | 12 kHz | 1 <sup>st</sup> target velocity           | -10 m/s |
| Platform velocity              | 90 m/s | 1 <sup>st</sup> target position           | 90°     |
| Platform altitude              | 3 km   | 1 <sup>nd</sup> target SNR                | 30 dB   |
| Slant range                    | 10 km  | 2 <sup>nd</sup> target velocity           | 50 m/s  |
| Look direction                 | 90°    | 2 <sup>nd</sup> target position           | 100°    |
| The number of antenna          | 12     | 2 <sup>nd</sup> target SNR                | 35 dB   |
| The number of integrated pulse | 12     | 1 <sup>st</sup> jammer interference angle | 30°     |
| CNR                            | 40 dB  | 1 <sup>st</sup> jammer INR                | 25 dB   |
|                                |        | 2 <sup>nd</sup> jammerinterference angle  | 140°    |
|                                |        | 2 <sup>nd</sup> jammer INR                | 40 dB   |

### 3. SIMULATION AND DISCUSSION

The simulation has been conducted for the analysis of the GMTI performance using STAP algorithm. The simulation parameters are given in Table 1. Fig. 3 shows the clutter and jammer environments, where two targets and two jammers exist with a non-moving ground clutter. It is assumed that platform velocity is 90 m/s, the position of the first moving target exists at 90 degrees in azimuth, and velocity and SNR are -10 m/s and 30 dB, respectively. The second moving target with the SNR of 35 dB is located at the direction of the 100 degrees and the ground velocity is 50 m/s. The JNR (jammer-to-noise ratio) and incident angle of the first jammer are 25 dB and 30 degrees in azimuth, and second jammer are 40 dB and 140 degrees, respectively.

After rejecting the clutter and jammer simultaneously using STAP filtering, final detected ground target signal is shown in Fig 4. The filter weight is found to be optimum weight vector. The notch filter is generated along the ground clutter line, and the jammers incoming at 30 and 140 degrees are suppressed by the null filters at these angles. The second ground moving target can be detected after STAP filtering since the SNR loss is negligible. However, the SNR of the first moving target close to the ground clutter band is decreased by clutter notch filter. This may cause the desired target detection difficult, resulting in degradation of the probability of detection.

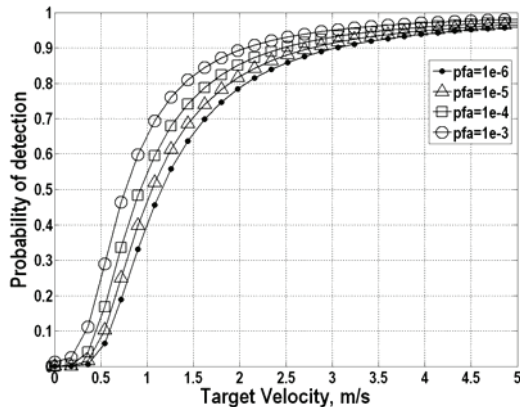


Figure 5. Minimum detectable velocity

The detection probability according to the velocity of ground moving target is illustrated in Fig 5. Since the amount of SNR loss is affected by the notch filter response in the target Doppler velocity, and thus the detection probability of target can be changed depending on the SNR loss. The symbols of the circle, square, triangular, and dot denote the detection probability with respect to the target velocity in the given false alarm rate of  $10^{-3}$ ,  $10^{-4}$ ,  $10^{-5}$ , and  $10^{-6}$ , respectively. In case of the false alarm rate of  $10^{-6}$ , the required SNR is 12.3 dB for the achieving the detection probability of 90%. Table 2 summaries the overall performance of the MDV in the function of the detection probability in the given false alarm rate. It is noted that the detectable velocity of the slow ground moving target using STAP ranges between 0.91 m/s and 3 m/s, from the relatively ideal airborne/spaceborne array radar platform.

#### 4. CONCLUSION

A space-time adaptive processing (STAP) can be effective for array radar in the airborne/spaceborne moving platform. In this paper, the characteristics of target, ground clutter and jammer signal are analyzed and designed to detect the slow ground moving target in two dimensional angle-Doppler domains. The simulation is performed for ground moving target detection by rejecting both clutter and jammer simultaneously through the STAP processing. The probability of target detection is presented in terms of SNR and the minimum detectable velocity in the given false alarm rate. The simulation results show that the MDV can be ideally achieved up to 2 m/s ~ 3 m/s at the 90% of detection probability in the given false alarm rate of  $10^{-6}$  to  $10^{-3}$ . It is noted that the detectable velocity of the slow ground moving target using STAP ranges between 0.91 m/s and 3 m/s, from the relatively ideal airborne/spaceborne array radar platform. This technique may be useful for the surveillance and traffic monitoring of moving vehicle on the road.

#### 5. REFERENCES

- [1] D. Cerutti-Maori, J.Klare, W.Burger, A.R. Brenner, J.H.G. Ender, "Wide area traffic monitoring with the PAMIR system", *IGARSS 2007*, pp.3567-3570, July 2007
- [2] Richard Klemm, *Principles of Space-Time Adaptive Processing*, IET, 2006

TABLE I. MDV according to False Alarm Rate and Detection Probability

| Detection probability | 90%      | 85%  | 80%  | 75%  | 70%  | 60%  |
|-----------------------|----------|------|------|------|------|------|
| False alarm rate      | MDV, m/s |      |      |      |      |      |
| $10^{-6}$             | 3        | 2.45 | 2.07 | 1.82 | 1.63 | 1.36 |
| $10^{-5}$             | 2.8      | 2.23 | 1.89 | 1.66 | 1.48 | 1.23 |
| $10^{-4}$             | 2.45     | 1.97 | 1.68 | 1.47 | 1.32 | 1.08 |
| $10^{-3}$             | 2.08     | 1.66 | 1.41 | 1.23 | 1.1  | 0.91 |